Scripta Materialia 154 (2018) 123–126

Contents lists available at ScienceDirect

Scripta Materialia

journal homepage: www.elsevier.com/locate/scriptamat

Regular article

# Grain refinement and amorphization in nanocrystalline NiTi micropillars under uniaxial compression

Peng Hua, Kangjie Chu, Qingping Sun *

*Department of Mechanical and Aerospace Engineering, The Hong Kong University of Science and Technology, Clear Water Bay, Hong Kong*

ARTICLE INFO

*Article history:*
Received 27 April 2018
Accepted 20 May 2018
Available online xxxx

*Keywords:*
Shape memory alloy
Grain refinement
Amorphization
Severe plastic deformation (SPD)
Cuboidal micropillar

ABSTRACT

Microscale plastic deformation mechanisms of nanocrystalline NiTi micropillars with an average grain size (GS) of 65 nm are investigated by uniaxial compression. Cuboidal NiTi micropillars with uniform cross-sectional area along the height are manufactured by focused ion beam. It is found that the plastic deformation of the micropillars under compression is realized by localized shear band formation with large strain bursts, leading to significant amorphization and GS reduction from 65 nm to as small as 11 nm in the shear band. The experiment indicates that microfabrication by severe plastic deformation could be a promising manufacturing technology.



NiTi shape memory alloys (SMAs) are widely-used in bio-medical implants [1,2] and micro-electro-mechanical systems (MEMS) [3]. Recently, nanocrystalline (nc) NiTi has drawn much research interests, as the nanocrystallization not only significantly enhances the thermal-mechanical properties but also improves the fatigue life of the material [4,5]. One of the traditional methods to obtain the nc microstructure is macroscale severe plastic deformation (SPD) like high pressure torsion, equal-channel angular extrusion and multi-axial forging which can impose a large plastic strain on the bulk materials [6–12]. With the development of microscale fabrication, microscale SPD (micro-SPD) could be a promising manufacturing technology for small size engineering. In such an endeavor, systematical experimental study of the micro-SPD is essential to this potential technology but has not been available in the literature so far.

In this letter, we first fabricate square cuboidal micropillars from a bulk nc NiTi sample with an average GS of 65 nm, and then uniaxially compress the micropillars up to a nominal compressive strain of 20.7%. We investigate the impact of a large plastic strain on the resulting microstructure of the micropillars. We finally discuss the underlying mechanisms of the microstructure changes in the micropillars and the implication of the experiment on the future development of micro-SPD in small-scale engineering.

A commercial superelastic NiTi sheet (Johnson Matthey Incorporation) with a chemical composition of 50.9 at. % Ni-49.1 at. % Ti and an austenite finish temperature of 287 K was used as raw material. A JEOL 2010 high resolution TEM was used to observe the microstructure of the undeformed NiTi sample. The nanoscale NiTi grains were in austenite phase (B2 cubic lattice [13]), as indicated by the selected area diffraction pattern (SADP) shown in Fig. 1a. The average GS of the original sample was 65 nm, as shown in Fig. 1b. A tapered cylindrical micropillar with a diameter of 5 $\mu m$ (Fig. 2a) was first fabricated and then milled to obtain flat faces (Fig. 2b) by using the focused ion beam (FIB) in a Helios G4 DualBeam (Thermo Fisher Scientific). A square cuboidal micropillar (Fig. 2c) was manufactured after milling four faces of the cylindrical pillar. By utilizing this method, two square cuboidal micropillars with an identical size of 1.67 $\mu m$ (edge length of the top face) and an aspect ratio (ratio of the height to the edge length of the top face) of 2.4 were fabricated. Compared with the widely-used tapered cylindrical micropillars (Fig. 2a), the cuboidal micropillars (Fig. 2c) have the advantages of uniform cross-sectional area along the height and very flat surfaces for a more convenient observation of surface morphology changes of the micropillar under compression. The micropillar was situated in a 20 $\mu m$-diameter circular cavity, leaving enough room for the indenter tip. A nanoindenter (Hysitron TI 950) equipped with a custom-made 10 $\mu m$ flat-end tip was used to compress the micropillars at the room temperature (~298 K). The compressive tests were set in displacement-control mode to have a nominal compressive strain rate of $2.5 \times 10^{-2}\ s^{-1}$ which was chosen to avoid the long-time drift problem of the nanoindenter [14,15]. The displacement control mode was favored as it provides a relatively constant displacement rate and controls the maximum displacement to avoid destroying the micropillars. The nominal engineering stress $\sigma$ and strain $\varepsilon$ were calculated using $\sigma = |P/A_0|$ and $\varepsilon = |\Delta h/h_0|$, where $P$, $\Delta h$, $h_0$ and $A_0$ are the compressive load, the height reduction, the original height and the cross-sectional area of the micropillars, respectively. The surface

* Corresponding author.
*E-mail address:* meqpsun@ust.hk (Q. Sun).

https://doi.org/10.1016/j.scriptamat.2018.05.034
1359-6462/

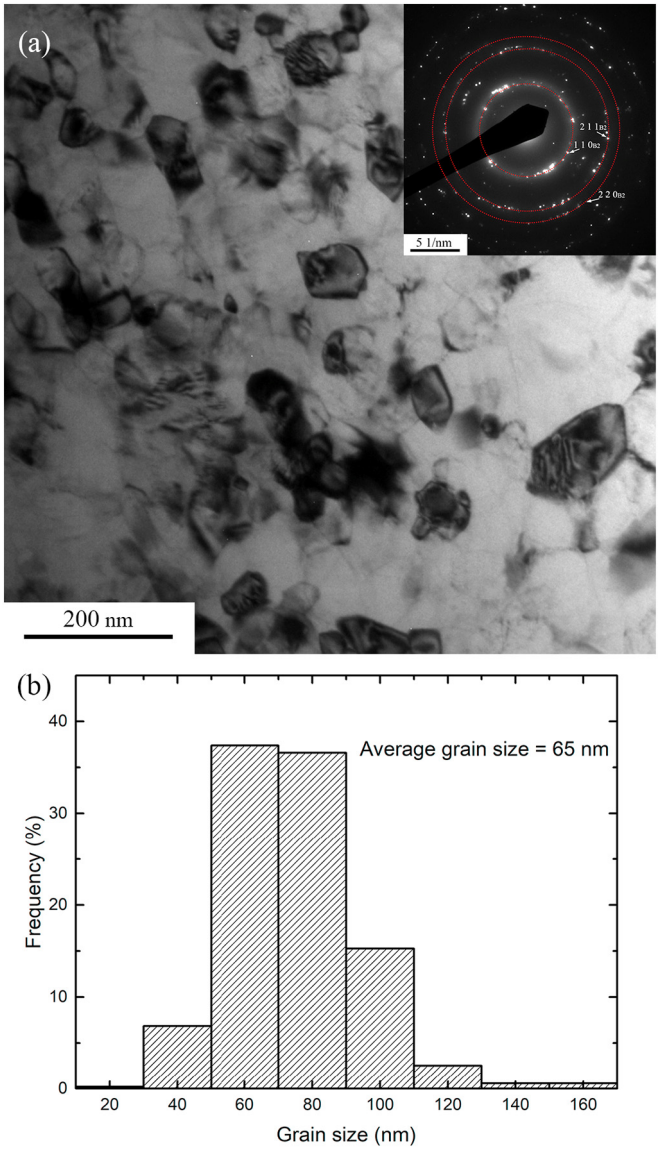


**Fig. 1.** (a) Bright-field TEM image of the undeformed NiTi sample where the inset shows the selected area diffraction pattern (SADP), and (b) grain size distribution of the original sample.

morphology of the plastically deformed micropillars were observed by the SEM after the compression. Post-mortem TEM samples were extracted from the plastically-deformed micropillars by lift-out technology.

The superelastic stress-strain curve of the NiTi micropillar loaded well below the yield strength (2.1 GPa as shown in Fig. 3b) is plotted in Fig. 3a. The superelastic behavior of NiTi originates from the reversible phase transformation between B2 austenite and B19′ martensite during loading and unloading [13]. The micropillar under compression is firstly elastically deformed (stage I in Fig. 3a) up to $\sigma_{forward}$ (~600 MPa) beyond which stress-induced martensitic transformation takes place (stage II). After the phase transformation is complete, the martensite phase is further detwinned and elastically deformed (stage III). Since the maximum stress is below the yield strength of the martensite phase (2.1 GPa as shown in Fig. 3b), unloading the micropillar leads to a complete recovery of strain through elastic unloading of martensite phase (stage IV), reverse transformation from B19′ to B2 (stage V) and elastic unloading of austenite (stage VI).

The full stress-strain curve of the micropillar that is compressed to the nominal strain of 20.7% is shown as the blue-dotted curve in Fig. 3b. It is seen that the martensite phase undergoes large irreversible plastic deformation when the applied stress reaches the yield strength of 2.1 GPa. The stress-strain curve in the plastic deformation stage shows a typical feature of plastic deformation instability with several large strain bursts as shown by the dotted regions. The corresponding strain and strain rate against the time are plotted in Fig. 3c where the sudden jumps in the strain and strain rate correspond to the strain bursts [16]. The time interval between two neighboring dots in Fig. 3b is 0.005 s. As set by the nanoindenter program to protect the sample and the nanoindenter tip from damage, the micropillar is partially unloaded by the nanoindenter to decrease the amount of compression after each strain burst. Then, the micropillar is elastically reloaded until reaching a higher critical stress for the next strain burst. This unloading-reloading feature is common in microscale compression tests under displacement control [17], and it does not affect the nature of the unstable plastic deformation process.

The surface morphology of the plastically-deformed cuboidal micropillar is shown in Fig. 4a. It is seen that the top part of the micropillar slides down along 45° shear plane during the compression, forming a localized shear band (containing many individual slip and sliding events) between the top and the bottom part of the micropillar. As shown in the bright-field TEM image (Fig. 4b), the shear band is oriented at an angle of 45° to the loading direction, i.e. the shearing occurs along the direction of the maximum shear stress. The microstructure in the localized shear band differs significantly from the rest part of the micropillar. Inside the shear band (Fig. 4c), the microstructure consists of amorphous phase and significantly refined grains with sizes as small as 11 nm, much smaller than the average GS of the rest part of the micropillar (65 nm). The SADP of the shear band (Fig. 4c) shows that the austenite (B2 lattice), martensite (B19′ lattice [13]) and amorphous phases coexist in the shear band. The microstructure change might explain why the critical stress for strain burst increases with the strain (Fig. 3b), as the refined 11 nm grains are more resistant to plastic deformation than the original 65 nm grains [18].

A schematic drawing of the localized plastic deformation of the nc NiTi micropillar is shown in Fig. 4d. The total vertical displacement of the strain bursts in the stress-strain curve of Fig. 3b is 337 nm (obtained from the load-displacement curve) which is close to the observed

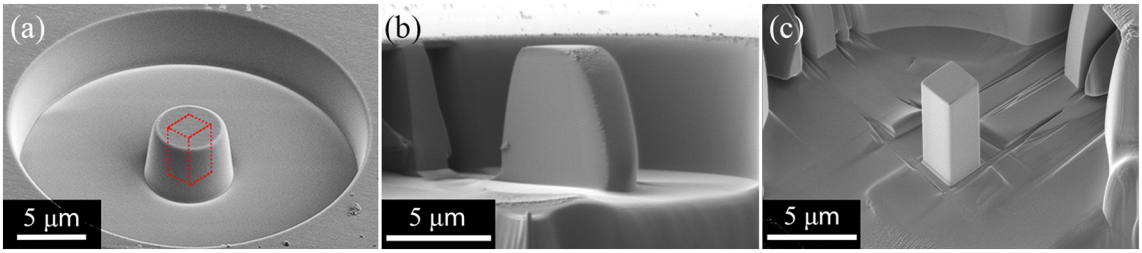


**Fig. 2.** (a) A cylindrical micropillar, (b) two parallel faces of the cylindrical pillar were milled by the FIB, and (c) the final cuboidal micropillar.